Bol. Soc. Paran. Mat.
©SPM – E-ISSN-2175-1188
SPM: www.spm.uem.br/bspm

(3s.) **v. 2025 (43)** : 1–17.
ISSN-0037-8712
doi:10.5269/bspm.75837

Dynamical Behaviorism of Hepatitis B Epidemic Model with Crowley-Martin Perspective

Thangavel Megala, Thangaraj Nandha Gopal, Yasir Khan*, Manickasundaram Siva Pradeep, Muthuradhinam Sivabalan, and Arunachalam Yasotha

ABSTRACT: Hepatitis B Virus (HBV) is a major global health threat, causing chronic liver inflammation, cirrhosis, and liver cancer. This study develops a novel epidemic model integrating a constant vaccination strategy, where susceptible individuals are immunized at a fixed rate due to vaccination, reducing the risk of infection. The model incorporates the Crowley-Martin functional response to capture nonlinear transmission dynamics. We analyze the dynamical behaviour, focusing on the basic reproduction number (R_N) and their stability properties. We establish the global asymptotic stability of Hepatitis-free equilibrium, ensuring the system remains disease-free when $R_N < 1$. Also, transcritical bifurcation occurs when $R_N = 1$ marks the threshold between disease eradication. For $R_N > 1$, we prove the global stability of the endemic equilibrium using Dulac's criteria. The sensitivity analysis of R_N helps us understand which parameters have the biggest impact on disease transmission. In numerical simulations we use Non-Standard Finite Difference (NSFD) scheme to validate our findings, with phase-plane analysis at $h = 0.1$ showing greater accuracy compared to traditional methods such as Runge-Kutta (RK4) and Euler, effectively capturing the model's long-term dynamics.

Key Words: HBV model, stability, vaccination rate, equilibrium point.

Contents

1. Introduction

Hepatitis B Virus (HBV) represents a major public health concern, affecting over 290 million chronically infected worldwide [1]. As a major cause of liver infection, including cirrhosis and hepatocellular carcinoma, understanding the dynamics of HBV transmission and infection is crucial for effective public health interventions and treatment strategies. The virus is primarily transmitted through contact with infectious body fluids, and its chronic form can lead to severe long-term health complications [2,3,4]. HBV can cause a severe and potentially life-threatening liver disease. It is a DNA virus that belongs to the Hepadnaviridae family of viruses [5,6]. Mathematical modeling has emerged as a powerful tool in epidemiology, providing insights into the complex interactions between the virus, host immune responses, and various risk factors associated with transmission. By simulating the dynamics of HBV infection, researchers can explore the effects of different intervention strategies, such as vaccination, antiviral therapies, and public health policies, on disease prevalence and transmission rates. This study aims to develop

* Corresponding author.
2010 *Mathematics Subject Classification:* 92B05, 92C80.
Submitted February 23, 2025. Published September 25, 2025

a comprehensive mathematical model of HBV infection that incorporates key biological and epidemiological factors. By analyzing the model's dynamics, we seek to identify critical parameters that influence the spread of the virus and assess the potential impact of various control measures. Our ultimate aim is to enhance the understanding of HBV epidemiology and to guide strategies aimed at reducing the impact of this preventable disease. At 2013 World Health Organization, the global health impact report on viral hepatitis indicates that chronic liver disease caused by HBV and HCV affects over 240 million and 150 million individuals, respectively. Africa ranks second, after Asia, in the number of chronic HBV carriers and is acknowledged as a region with significant endemicity [7,8]. Ethiopia has a high prevalence of hepatitis virus, which includes infections caused by viruses such as Hepatitis B and C. [9]. This neglect can lead to increased morbidity and mortality associated with chronic liver disease, as well as a lack of awareness and education about the disease among the population. Significant research has been carried out to create both stochastic and deterministic models that describe the dynamics of infectious disease spread and surface antigen [10,11,12,13,14,15]. Also, the Hattaf-Yousfi incidence rate of $\frac{\beta SI}{\gamma_0+\gamma_1 S+\gamma_2 I+\gamma_3 SI}$ [42,43] generalizes numerous types of incidence rate like the bilinear incidence, the saturation incidence, the Beddington-DeAngelis incidence rate, and the Crowley-Martin incidence rate.

Regular monitoring of liver health in individuals with chronic HBV can help in early detection of complications, such as cirrhosis or liver cancer. This proactive approach is vital for improving long-term health outcomes. The Hepatitis B vaccine is made from a non-infectious part of the virus, specifically the surface antigen (HBsAg). It is produced using recombinant DNA technology, where the gene for the HBsAg is inserted into yeast or mammalian cells, which then produce antigen. The vaccine demonstrates high efficacy, successfully preventing over 90 percent viruses in immunized individuals. Also greatly lowers the chance of developing chronic HBV and its complications, including liver cirrhosis and cancer [16]. The standard vaccination schedule typically consists of three doses:

The first dose is administered at birth or as soon as possible afterward. The second dose follows 1 to 2 months later, and the third dose is given 6 months after the initial dose. Different vaccination schedules may be applied for particular groups, including adults or people with a higher risk of infection. The vaccine is recommended for all infants, children, and adolescents, as well as adults at high risk for HBV infection, including healthcare workers, individuals with multiple sexual partners, and those with chronic liver disease [17,18,19]. McKendrick and Kermack established SIR model in 1927, making it one of the simplest and most used models in epidemiology [20]. In this paper, we will develop a predictable approach for HBV spread using the fundamental assumptions of the traditional SIR model. In epidemiology, models often in the various incidence rate, which measures the new infections during a particular time and plays a key role in understanding the dynamics of disease transmission.

Kermack and McKendrick's SIR model represents disease dynamics using three compartments: susceptible (S), infected (I), and recovered (R). The incidence rate of new infections is given by βSI, where β is the transmission rate, indicating that new infections occur through interactions between susceptible and infected individuals. This model effectively captures how an infectious disease spreads within a population and how those dynamics change over time. It is generally called bilinear incidence or mass action [21,22,23]. The standard incidence rate in epidemiological models is expressed as $N\beta SI$, where N is the total population size. While this bilinear incidence rate works under stable population conditions, it diverges when population size varies, particularly with increased disease exposure risk. May and Anderson [24] investigated a modified incident rate $\frac{\beta SI}{1+\gamma_1 S}$, accounting for epidemic control measures through the saturation term γ_1. Similarly, Capasso and Serio [25] proposed another variant, $\frac{\beta SI}{1+\gamma_2 I}$, where the denominator captures the behavioral changes and crowding effects in susceptible individuals caused by the infected population. These adjustments enhance the realism of disease spread models in varying population dynamics. The Beddington–DeAngelis (BD) form of non-linear incidence rate, denoted as $\frac{\beta SI}{(1+\gamma_1 S+\gamma_2 I)}$, was independently proposed in 1975 by Beddington [26] and DeAngelis [27]. This incidence rate has been adopted by many researchers in their epidemiological models in later studies. Hattaf et al [44] investigated a delayed SIR (Susceptible-Infected-Recovered) epidemic model that incorporates a generalized incidence rate, where the time delay represents the incubation period of the disease. The study focuses on determining the threshold parameter $R_0(\tau)$, which indicates whether the disease will become extinct or persist in the population. Additionally, the author employs Lyapunov functional techniques to establish the global stability of both the disease-free equilibrium and the endemic equilibrium within the

model. Our model extends the approach in [44] by incorporating a more generalized incidence function.

Kaddar [28,29] introduced a delayed model that incorporates Beddington–DeAngelis incidence rate. They demonstrated significant values of the inhibitory effect. Therefore, inspired by the preceding discussion, this work employs a new rate called Crowley-Martin perspective [30]. It is typically represented as a nonlinear function that reflects the interactions between healthy and diseased individuals. The equation is expressed as $\frac{\alpha SI}{(1+\eta S)(1+\mu I)}$ with α as a transmission rate. However, Kaddar [28,29] does not specify the stage of infection. Moreover, the model does not account for the vaccination rate. Building on this observation, the present study adopts a different approach by employing Crowley-Martin perspective. In addition, vaccination plays a vital role in controlling the propagation of infectious pathogens within a population. To address this, a vaccination (Γ) is introduced in the system, enhancing its ability to accurately represent infection dynamics and disease progression. Also, some researchers have explored epidemic model with vaccination [31,32]. Other examiner use Crowley-Martin perspective in Eco-epidemiological model to analysis stability [33,34,47]. In most cases, systems consisting of non-linear differential or difference equations are used to develop epidemiological models. Several methods can be used to discretize a model that is represented by a nonlinear system of differential equations. As many of the continuous dynamical model features must be preserved as much as feasible in the discretized model. Runge-Kutta and Euler procedures, as well as a few other finite-difference methods, are popular discretization techniques. Unfortunately, these techniques can sometimes lead to unfavorable dynamic patterns, including the appearance of oscillatory cycles or numerical instabilities [35,36]. Discretizing the equation helps identify inaccuracies when comparing numerical simulation results. Mickens [37,38] introduced an innovative technique known as non-standard finite difference (NSFD) method to overcome these challenges. Recent studies [44,45,46] have explored the role of memory effects in disease dynamics using fractional-order derivatives, such as the Hattaf mixed fractional derivative and fractal-fractional derivative. These approaches can capture long-term dependencies in infection progression, making them valuable for modeling chronic diseases like HBV. While our study employs classical time derivatives for analytical tractability and ease of comparison with existing models, incorporating fractional derivatives remains a potential future direction to enhance the model's realism.

In this paper, we provide Hepatitis model that contains a Crowley-Martin perspective, together with treatment and vaccination strategies. Our study addresses a gap in the literature, as no previous research has explored the impacts of vaccination and Crowley-Martin incidence rate are examined. We focus on a Hepatitis epidemiological model that is more comprehensive than those previously proposed. By analyzing its continuous structure, we aim to better understand how vaccination strategies and the Crowley-Martin incidence rates impact the spread of Hepatitis, providing insights that can enhance public health interventions and strategies. Initially, we performed a dynamical study to determine the presence of positive solutions to the proposed model, discovering both free of disease and endemic states. The basic reproduction number, R_N, was computed using the next-generation matrix. We then used the linear stability theorem to examine the model's locallly asymptotic stability (LAS), and we use Poincaré-Bendixson theorem to analyze its global asymptotic stability. The existence of a transcritical bifurcation was also confirmed. Following this, we created a NSFD numerical scheme by Mickens' technique. We investigated the stability features of the continuous HBV model to determine their dynamical consistency. Finally, we conducted numerical simulations to support our theoretical findings, demonstrating the efficiency of the proposed model in capturing HBV dynamics of transmission under the defined parameters.

The structure of the work is organized into various key divisions that systematically address HBV model. In Section 2, we introduce the mathematical formulation of the model (2.1), along with the assumptions that underlie its structure. This foundational analysis lays the groundwork for exploring the model's behavior. Section 3 is devoted to establishing the well-posedness of the model by proving that the solutions remain non-negative and bounded, thereby ensuring its biological relevance. Section 4 focuses on the existence of equilibrium points by deriving the secondary infection and finding the Hepatitis-free equilibrium (HFE). Furthermore, we construct and analyze theorems related to the local and global asymptotic stability (LAS and GAS) of the HFE, offering insights into the system's stability under different scenarios. Section 5 extends this analysis to the endemic equilibrium (EE), examining both LAS and GAS to deepen our understanding of the model's long-term dynamics. Additionally, we investigate the occurrence of a transcritical bifurcation at $R_N = 1$. In Section 6, we perform a sensitivity

analysis of the basic reproduction number to identify key parameters influencing disease transmission. This is complemented by numerical simulations that validate the theoretical results and provide practical insights into the model's implications. Section 7 concludes with a summary of the main findings and suggests directions for future research. Fig 1 presents a schematic representation of the Hepatitis B model, visually capturing the interactions.

2. Model Formulation

Let $\mathcal{N}(t)$ refers to the overall population size at a given time t, which is categorized as three groups: susceptible, diseased and recovered population, represented as $S(t)$, $I(t)$, and $R(t)$, respectively. Therefore, we can express the total population as $N(t) = S(t) + I(t) + R(t)$. This model incorporates several key elements to simulate the dynamics of disease within a population. It features a fixed recruitment rate, allowing new susceptible individuals to enter the population at a constant rate, which represents births or new arrivals. The incidence rate, calculated using the Crowley-Martin framework, measures how quickly susceptible individuals become infected based on their interactions. Additionally, the model includes vaccination for some susceptible individuals, which reduces the pool of those who can contract the disease. Mortality rates are also accounted for, encompassing both disease-related deaths from the infection and natural deaths from other causes. Furthermore, the model posits that certain infected individuals may recover on their own without medical intervention, depending on their physical strength. Together, these components create a comprehensive framework for understanding disease spread and evaluating the impact of interventions like vaccination on overall population health.

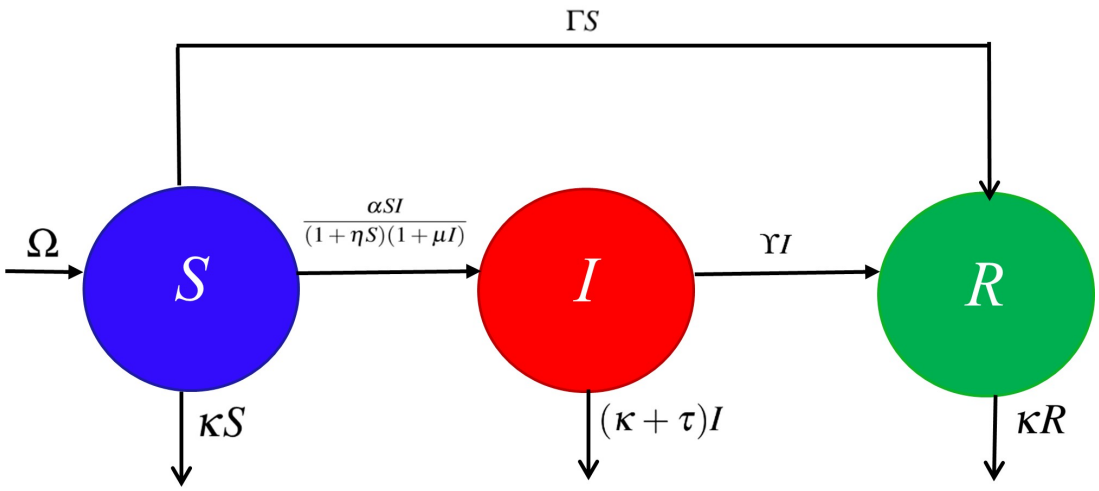

Figure 1: Block Diagram of the HBV Epidemic Framework

- The model begins with biologically feasible population values, recognizing that negative population sizes are not meaningful, as a population cannot consist of fewer than zero individuals. The notation $S(0)$, $I(0)$, *and* $R(0)$ represents the initial counts of susceptible, infected, and recovered individuals, respectively.
- The newborns are typically born without immunity to diseases. Therefore, they are categorized as susceptible until they either become infected or are vaccinated.
- The level of incidence is expected to correlate with the Crowley-Martin perspective. This model accounts for the effects of both the density of uninfected population and the infected population on the rate of new infectives.
- Individuals who are vaccinated and acquire immunity move from the susceptible class to the recovered class, illustrating that vaccination not only shields individuals from infection but also enhances

Table 1: Epidemiological interpretation of variables in the HBV model with their respective units

Variables	Epidemiological Interpretation	Units
S	Susceptible HBV Population	Individuals
I	Diseased HBV Population	Individuals
R	Recovered HBV Population	Individuals
Ω	Recruitment rate	Individuals per unit time
α	Disease transmission rate	Per unit time
η	Preventive measures	Dimensionless
R_N	Basic reproduction number	Dimensionless
Γ	Constant Vaccination rate	Per unit time
μ	Infected individuals undergoing treatment	Per unit time
κ	Natural death rate of susceptible populations	Per unit time
Υ	Infected individuals receiving treatment	Per unit time
τ	Disease-induced mortality rate	Per unit time

the population's overall immunity.

- Once individuals recover from the infection, they gain lasting immunity and cannot be reinfected. This is a critical aspect of many infectious disease models, as it influences the dynamics of disease spread and the potential for future outbreaks. Permanent immunity simplifies the model by removing recovered individuals from the susceptible pool. Table 1 shows the detailed interpretation of Hepatitis B Virus model.

Taking into account of all the rules, assumptions and flow chart, the nonlinear differential equation of Hepatitis B Virus system can be expressed as:

$$\begin{aligned}
\frac{dS}{dt} &= \Omega - (\Gamma + \kappa)S - \frac{\alpha SI}{(1+\eta S)(1+\mu I)}, \\
\frac{dI}{dt} &= \frac{\alpha SI}{(1+\eta S)(1+\mu I)} - (\tau + \kappa + \Upsilon)I, \\
\frac{dR}{dt} &= \Upsilon I - \kappa R + \Gamma S.
\end{aligned} \tag{2.1}$$

with t

$$S(0) = S_0 > 0,\ I(0) = I_0 > 0\ and\ R(0) = R_0 > 0.$$

3. Well-Posedness

Within the region $\mathbb{R}^3_+$, HBV model (2.1) ensures that all solutions remain positive for $t \geq 0$, and the system's solutions are also bounded. By summing the three equations of the model, we obtain the following result based on population conservation principle:

$$\frac{dN}{dt} = \Omega - \kappa N - \tau I \leq \Omega - \kappa N \tag{3.1}$$

we get,

$$N(t) \leq \frac{\Omega}{\kappa} + \left(N(0) - \frac{\Omega}{\kappa}\right) e^{-\kappa t},\ \limsup_{t\to\infty} N(t) \leq \frac{\Omega}{\kappa} \tag{3.2}$$

where $N(t) = S(t)+I(t)+R(t)$ denotes the total population involved in the Hepatitis B dynamics. Based on these results, it is sufficient to analyze the Hepatitis B Virus model (2.1) within the specified region.

$$\Psi = \left\{(S, I, R) \in R^3_+ : S + I + R \leq \frac{\Omega}{\kappa}\right\}.$$

In HBV model (2.1), the first two equations describe the dynamics of the system without relying on the third equation. This means that the behavior and interactions represented by the first two equations can be understood and analyzed independently of the third equation's influence. By excluding the third equation, the model becomes simpler and more manageable, allowing researchers to focus on the essential dynamics of the disease spread and treatment without the added complexity of the third equation.

$$\begin{aligned} \frac{dS}{dt} &= \Omega - (\Gamma + \kappa)S - \frac{\alpha SI}{(1+\eta S)(1+\mu I)}, \\ \frac{dI}{dt} &= \frac{\alpha SI}{(1+\eta S)(1+\mu I)} - (\tau + \kappa + \Upsilon)I. \end{aligned} \tag{3.3}$$

with the conditions as

$$S(0) = S_0 > 0, \ I(0) = I_0 > 0.$$

We will carry out our analysis in the following regions:

$$\Psi = \left\{ (S, I) \in R_+^2 : S + I \leq \frac{\Omega}{\kappa} \right\}$$

4. Stability of hepatitis-free equilibrium state

It is clear that the system always has a Hepatitis-Free Equilibrium (HFE) point by setting the right-hand side of the system in the simplified Hepatitis B Virus model (3.3) to zero and considering $I = 0$.

$$E_0 = (S_0, I_0) = \left(\frac{\Omega}{\Gamma + \kappa}, 0 \right) \tag{4.1}$$

The reproduction number (R_N) represents the next generation matrix (NGM) of spectral radius [39,40]. The NGM is obtained by multiplying the transmission matrix and the removal matrix inverses:

$$R_N = \frac{\alpha\Omega}{(\Gamma + \kappa + \eta\Omega)(\kappa + \Upsilon + \tau)} \tag{4.2}$$

This is the reproduction number (R_N) for the given system. Note that R_N denotes the average number of secondary infections caused by a single infected individual in an entirely susceptible population. When $R_N > 1$, the infection can invade and persist in the population, whereas if $R_N < 1$, the disease will die out.

Theorem 4.1 *The Hepatitis-Free Equilibrium (HFE) point E_0 of model (3.3) remains stable if $R_N < 1$, but loses stability when $R_N > 1$.*

Proof: The jacobian form of the model (3.3) is

$$J(E_0) = \begin{bmatrix} -(\Gamma + \kappa) & -R_N(\kappa + \Upsilon + \tau) \\ 0 & (R_N - 1)(\kappa + \Upsilon + \tau) \end{bmatrix}$$

Solving for λ, we get two eigenvalues:

$$\lambda_1 = -(\Gamma + \kappa); \quad \lambda_2 = (R_N - 1)(\kappa + \Upsilon + \tau)$$

These are the eigenvalues of the Hepatitis-free equilibrium point. Note that the stability of the equilibrium point depends on the values of R_N and the other parameters. If $R_N < 1$, the equilibrium point is stable, and if $R_N > 1$, the equilibrium point is unstable. At $R_N = 1$, it undergoes transcritical bifurcation. □

Theorem 4.2 *For $R_N < 1$, the Hepatitis-Free Equilibrium (HFE) point E_0 of model (3.3) attracts all solutions, indicating that it is globally asymptotically stable.*

Proof: If $R_N < 1$, the only equilibrium point present is the Hepatitis-free equilibrium point E_0. Furthermore, as indicated in (3.3), the non-negative solution of the system (3.3) is bounded, with the S-axis being positively invariant and the I-axis repelling any positive solutions. Since E_0 is LAS, the Bendixson Theorem suggests that all non negative solutions of the system will tend toward E_0 as the time progresses towards infinity. Hence, the Hepatitis-free equilibrium point E_0 is GAS. This completes the proof. □

5. Stability of hepatitis endemic equilibrium state

Finding the endemic equilibrium points involves setting the equations to zero and solving the Hepatitis population variables, which helps us understand the long-term behavior of the disease within the population. Where, $E^* = (S^*, I^*)$,

$$\begin{aligned} S^* =& \frac{\kappa + \Upsilon + \tau + \mu\Omega}{\mu(\Gamma + \kappa) + \alpha - \eta(\kappa + \Upsilon + \tau)} \\ =& \frac{\Omega(\kappa + \Upsilon + \tau + \mu\Omega)}{\mu\Omega(\Gamma + \kappa) + (\kappa + \Upsilon + \tau)[R_N(\Gamma + \kappa) + \eta\Omega(R_N - 1)]}, \\ I^* =& \frac{(\Gamma + \kappa + \eta\Omega)(R_N - 1)}{\alpha - \eta(\kappa + \Upsilon + \tau) + \mu(\Gamma + \kappa)} \\ =& \frac{\Omega(\Gamma + \kappa + \eta\Omega)(R_N - 1)}{\mu\Omega(\Gamma + \kappa) + (\kappa + \Upsilon + \tau)[R_N(\Gamma + \kappa) + \eta\Omega(R_N - 1)]}. \end{aligned}$$

If $R_N > 1$, then the hepatitis endemic equilibrium exists.

Theorem 5.1 *The Hepatitis endemic equilibrium state (S^*, I^*) is LAS when, $R_N > 1$ in the HBV model (3.3).*

Proof: We assume that $R_N > 1$ it indicates that the disease is capable of spreading within the population, leading to the possibility of an endemic state. To analyze the stability of this endemic equilibrium point, denoted as E^*, we can use the Jacobian matrix.

$$J(E^*) = \begin{pmatrix} -\frac{(\alpha-\eta x)[\alpha\Omega - x(y+\eta\Omega)]}{(x+\mu\Omega)\alpha} - y & -\frac{[\alpha+\mu(b+\eta\Omega)]x^2}{(x+\mu\Omega)\alpha} \\ \frac{(\alpha-\eta x)[\alpha\Omega - x(y+\eta\Omega)]}{(x+\mu\Omega)\alpha} & \frac{[\alpha+\mu(y+\eta\Omega)]x^2}{(x+\mu\Omega)\alpha} - x \end{pmatrix}$$

where, $x = \kappa + \Upsilon + \tau$, $y = \Gamma + \kappa$. To determine the stability of the equilibrium point E^* using the Jacobian matrix $J(E^*)$, we need to analyze its eigenvalues. The conditions for the eigenvalues to be negative are given by $Tr(J(E^*)) < 0$, and $det(J(E^*)) > 0$. Thus,

$$\mathrm{Tr}(J^*) = -\frac{x^2(y + \eta\Omega)(R_N - 1)[R_N y + (R_N - 1)\eta\Omega + \mu\Omega]}{\alpha\Omega(x + \mu\Omega)} - y.$$

$$\det(J(E^*)) = \frac{(R_N - 1)x^2(y + \eta\Omega)[R_N xy + (R_N - 1)x\eta\Omega + \mu y]}{\alpha\Omega(x + \mu\Omega)}.$$

Clearly, if $R_N > 1$, then the trace of $J(E^*)$ is negative, while the determinant is positive. This indicates that the equilibrium point of the syystem (3.3) is locally asymptotically stable (LAS). Therefore, the proof is complete, as required. □

Theorem 5.2 *If $R_N > 1$, the HBV model described by (3.3) is globally asymptotic stable (GAS) in the region Ψ.*

Proof: Assume $R_N > 1$. Considering the functions $m(S, I)$ and $n(S, I)$, RHS of the system (3.3). We define the Dulac function as follows: $X(S, I) = I^{-1}$. With this definition, we can proceed to analyze the behavior of the system using the Dulac criterion.

$$\frac{\partial(Xm)}{\partial S} + \frac{\partial(Xn)}{\partial I} = -\frac{\alpha(1 + \mu I)}{[(1 + \eta S)(1 + \mu I)]^2} - \frac{\Gamma + \kappa}{I} - \frac{S\mu\alpha}{[(1 + \eta S)(1 + \mu I)]^2} < 0.$$

for all $(S, I) \in \Psi$. Therefore, the system (3.3) does not exhibit any periodic orbits within the region Ψ. Given that the model (3.3) are bounded and that E_0 acts as an unstable saddle point when $R_N > 1$. So, we can apply the Poincaré-Bendixson theorem to conclude that the endemic equilibrium E^* is GAS, This completes the proof. □

6. Sensitivity Analysis

To determine the impact of each parameter on the basic reproduction number R_N, we use the forward sensitivity index, defined as:

$$\rho_x = \frac{\partial R_N}{\partial x} \times \frac{x}{R_N},$$

where x is any parameter in the expression for R_N:

$$R_N = \frac{\alpha\Omega}{(\Gamma + \kappa + \eta\Omega)(\kappa + \Upsilon + \tau)}.$$

We now compute the sensitivity indices for each parameter.

$$\frac{\partial R_N}{\partial \alpha} = \frac{\Omega}{(\Gamma + \kappa + \eta\Omega)(\kappa + \Upsilon + \tau)}.$$

$$\rho_\alpha = \frac{\Omega}{(\Gamma + \kappa + \eta\Omega)(\kappa + \Upsilon + \tau)}.\frac{\alpha}{R_N}$$

$$\frac{\partial R_N}{\partial \Omega} = \frac{\alpha[\Gamma + \kappa]}{(\Gamma + \kappa + \eta\Omega)^2(\kappa + \Upsilon + \tau)}$$

$$\rho_\Omega = \frac{\partial R_N}{\partial \Omega}.\frac{\Omega}{R_N}$$

$$\frac{\partial R_N}{\partial \Gamma} = -\frac{\alpha\Omega}{(\Gamma + \kappa + \eta\Omega)^2(\kappa + \Upsilon + \tau)}.$$

$$\rho_\Gamma = \frac{\partial R_N}{\partial \Gamma}.\frac{\Gamma}{R_N}$$

$$\frac{\partial R_N}{\partial \kappa} = -\frac{\alpha\Omega[(\Gamma + 2\kappa + \eta\Omega + \Upsilon + \tau)]}{[(\Gamma + \kappa + \eta\Omega)(\kappa + \Upsilon + \tau)]^2}$$

$$\rho_\kappa = \frac{\partial R_N}{\partial \kappa}.\frac{\kappa}{R_N}.$$

$$\frac{\partial R_N}{\partial \eta} = -\frac{\alpha\Omega^2}{(\Gamma + \kappa + \eta\Omega)^2(\kappa + \Upsilon + \tau)}.$$

$$\rho_\eta = \frac{\partial R_N}{\partial \eta}.\frac{\eta}{R_N}$$

$$\frac{\partial R_N}{\partial \Upsilon} = -\frac{\alpha\Omega}{(\Gamma + \kappa + \eta\Omega)(\kappa + \Upsilon + \tau)^2}.$$

$$\rho_\Upsilon = \frac{\partial R_N}{\partial \Upsilon}.\frac{\Upsilon}{R_N}$$

$$\frac{\partial R_N}{\partial \tau} = -\frac{\alpha\Omega}{(\Gamma + \kappa + \eta\Omega)(\kappa + \Upsilon + \tau)^2}.$$

$$\rho_\tau = \frac{\partial R_N}{\partial \tau}.\frac{\tau}{R_N}$$

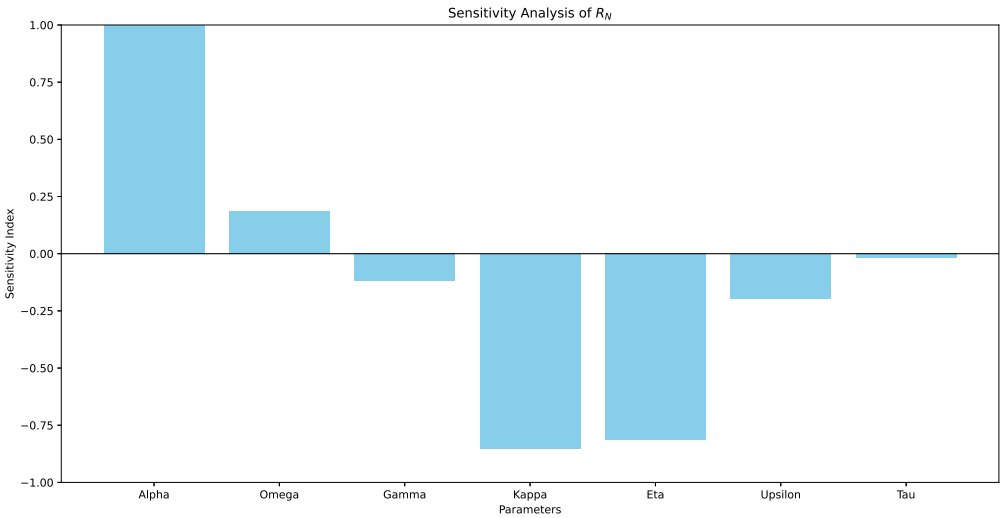

Figure 2: Sensitivity Index

The sensitivity analysis of R_N helps us understand which parameters have the biggest impact on disease transmission. (α) has the strongest positive influence, meaning that as it increases, the disease spreads more easily. (Ω) also has a positive effect, but to a lesser extent. On the other hand, (Γ), (κ), (η), and (Υ) have negative effects, meaning that increasing these values helps slow down transmission. (κ) and (η) play the most significant role in reducing R_N, making them key targets for disease control. (τ) has a small negative effect, suggesting it has a minor role in controlling the disease. (α) through vaccination and (κ) and (η) through treatment could be effective strategies. These results highlight the importance of limiting transmission and improving recovery rates to control hepatitis B. Understanding these influences helps in designing better intervention strategies. Figure (2) shows the sensitivity index for HBV infection.

7. Numerical Results

Numerical simulations play a crucial role in assessing how well mathematical models reflect real-world situations. This study presents numerical simulations to support the theoretical findings, focusing on two cases: a scenario in which $R_N < 1$, indicating disease eradication, and another where $R_N > 1$, suggesting potential disease spread. Using MATLAB R2017b, we compare three numerical methods—Euler, RK4 , and NSFD—to discretize and solve the HBV model. The results highlight the NSFD scheme's superior accuracy and stability, demonstrating its advantages over traditional methods.

Table 2: Control parametric values

Variables	Values	Source
Ω	6	estimated
α	0.01 or 0.03 or 0.1	estimated
η	0.8	[41]
Γ	0.7	estimated
μ	0.6	[41]
κ	0.4	estimated
Υ	0.1	estimated
τ	0.01	estimated

Case : 1 ($R_N < 1$) Table 2 lists the selected parameter value for this scenario. According to the data in Table 2, it is evident that $R_N = 0.017837 < 1$ and $E_0 = (0.909090901, 0)$.

Figure 3 compares the Euler and RK4 methods for the HBV model with initial values $S(0) = 1.0$, $I(0) = 0.7$, and time step $h = 0.1$. The top plot shows $S(t)$, and the bottom plot shows $I(t)$, with RK4 (solid red) proving more accurate than Euler (dashed blue). Maximum errors are 1.9929 for $S(t)$ and 0.0806 for $I(t)$, emphasizing RK4's better precision in capturing population dynamics.

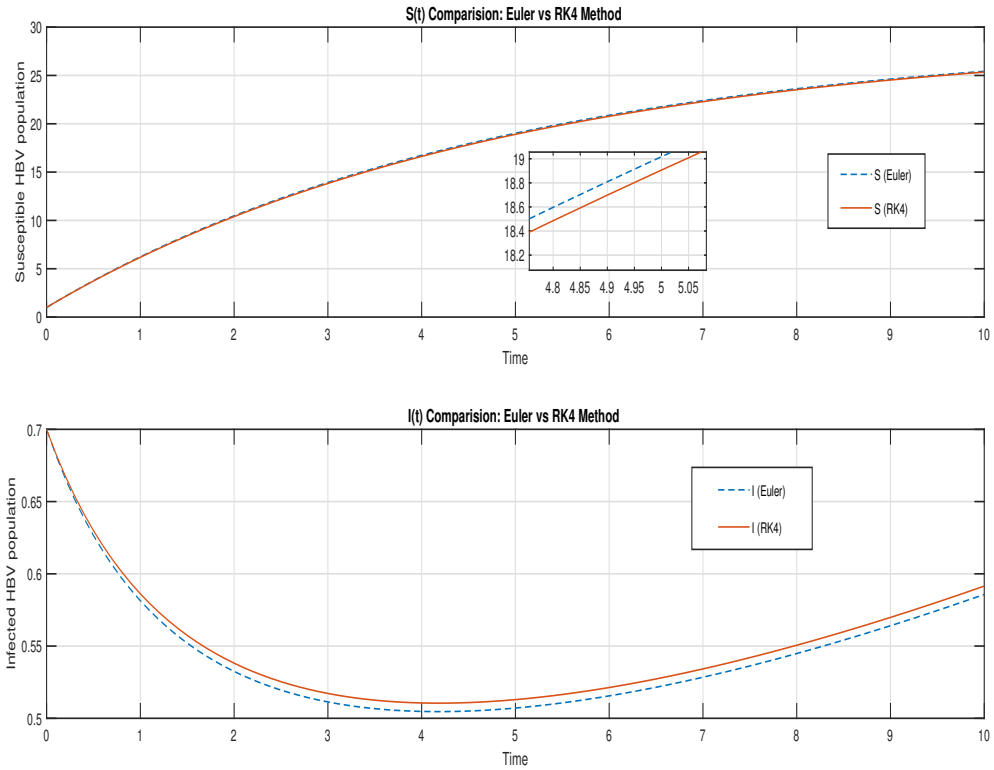

Figure 3: Comparison of HBV Population Dynamics using Euler and RK4 Methods for $S(0) = 1.0$ and $I(0) = 0.7$, with a time-step size of $h = 0.1$

Figure 4 compares NSFD (solid red) and RK4 (dashed blue) for HBV dynamics, showing $S(t)$ (top) and $I(t)$ (bottom). NSFD achieves higher accuracy, with maximum errors of 0.11113 for $S(t)$ and 0.00588 for $I(t)$ at $\alpha = 0.05$. While both methods show similar trends, NSFD captures rapid initial changes better and provides more consistent accuracy than RK4.

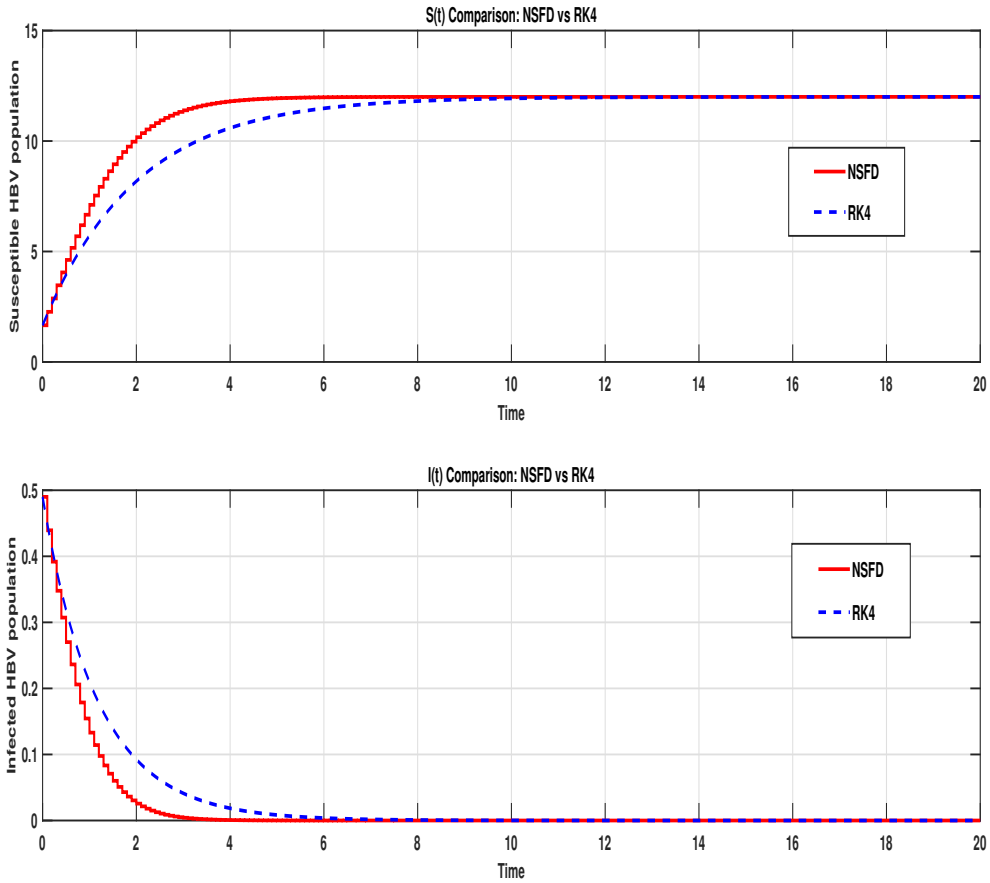

Figure 4: Comparison of HBV Population Dynamics using NSFD and RK4 Methods $S(0) = 1.0$ and $I(0) = 0.7$, with a time-step size of $h = 0.1$

Figure 5 shows that higher h values accelerate the decline of susceptible and infected populations, indicating faster disease control. For $h = 4$, the infected population drops to near zero quickly. The NSFD scheme accurately reflects this behavior, highlighting the impact of effective interventions like treatment or vaccination.

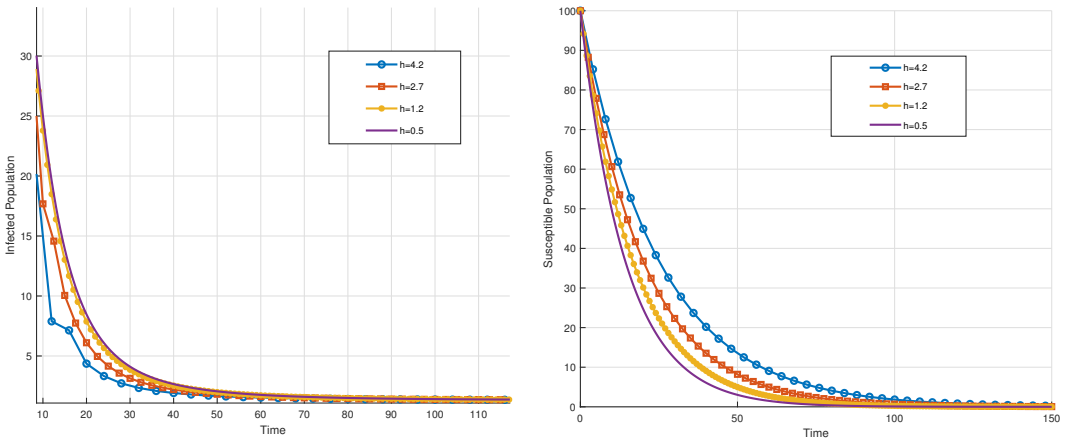

Figure 5: NSFD scheme numerical solutions for $h = 4,\ h = 2.5,\ h = 1$ *and* $h = 0.5$

Case : 2 ($R_N > 1$) Unlike the previous scenario, here $\alpha = 0.1$, while all other values remain identical. In this scenario, $R_N = 1.090 > 1$, and $E^* = (5.000458, 0.863945)$. Figure 6 shows GAS of E^* in the phase plane using NSFD scheme ($h = 0.1$). Trajectories from various initial conditions converge a stable endemic equilibrium, demonstrating the model's robustness and NSFD scheme's effectiveness in capturing long-term HBV dynamics.

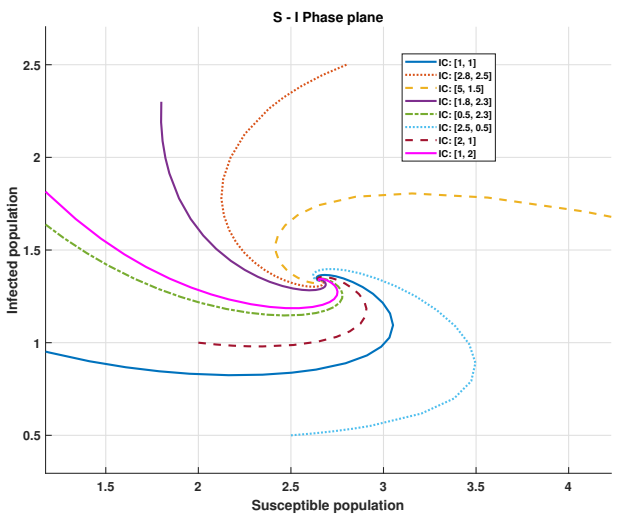

Figure 6: Global stability of Endemic equilibrium point of NSFD scheme with $h = 0.1$

Fig. 7 illustrates the impact of vaccination rates (Γ) on HBV dynamics. Higher Γ values increase the susceptible population and significantly reduce the infected population, with $\Gamma = 0.2$ showing the most effective control. Vaccination proves crucial in reducing infections and managing HBV spread.

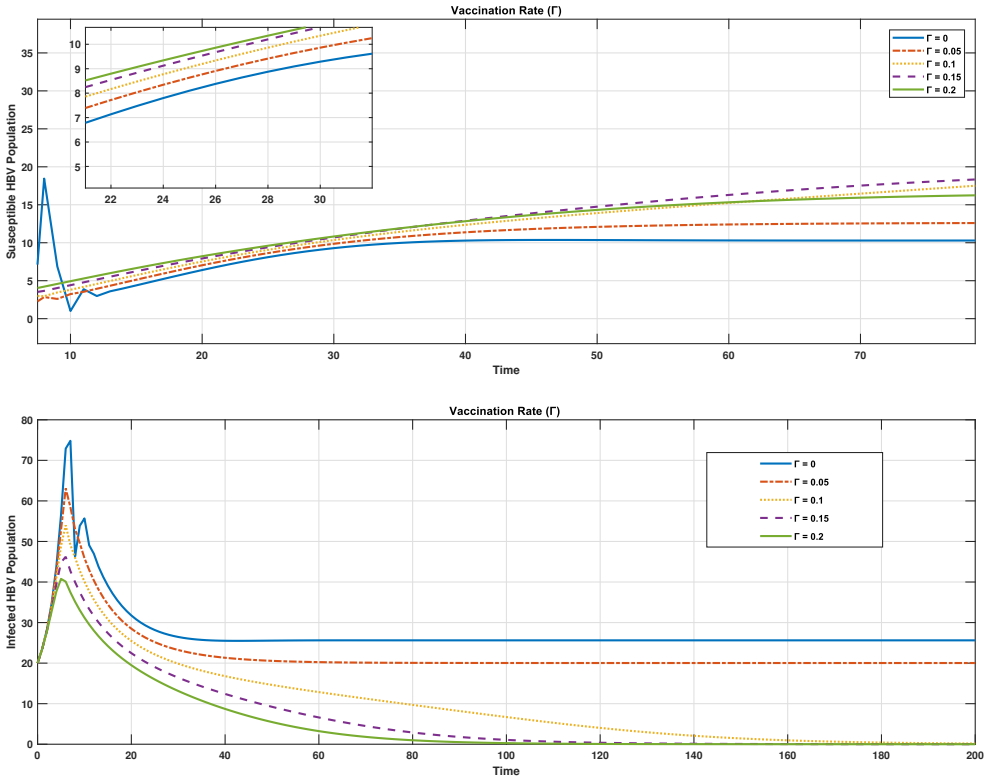

Figure 7: Variation of vaccination rate (Γ) on the dynamics of susceptible and infectious HBV Populations over time

Fig. 8 demonstrates how the reproduction number R_N changes with the transmission rate and recovery rate Υ. Higher values of α combined with lower values of Υ result in a high R_N, as seen in the red/yellow region on the right, indicating a greater likelihood of infection spread. Conversely, lower α and higher Υ correspond to a low R_N, represented by the blue region on the left, suggesting potential disease elimination. The transition zone, where R_N shifts from above to below 1, marks a critical threshold between outbreak scenarios and disease control.

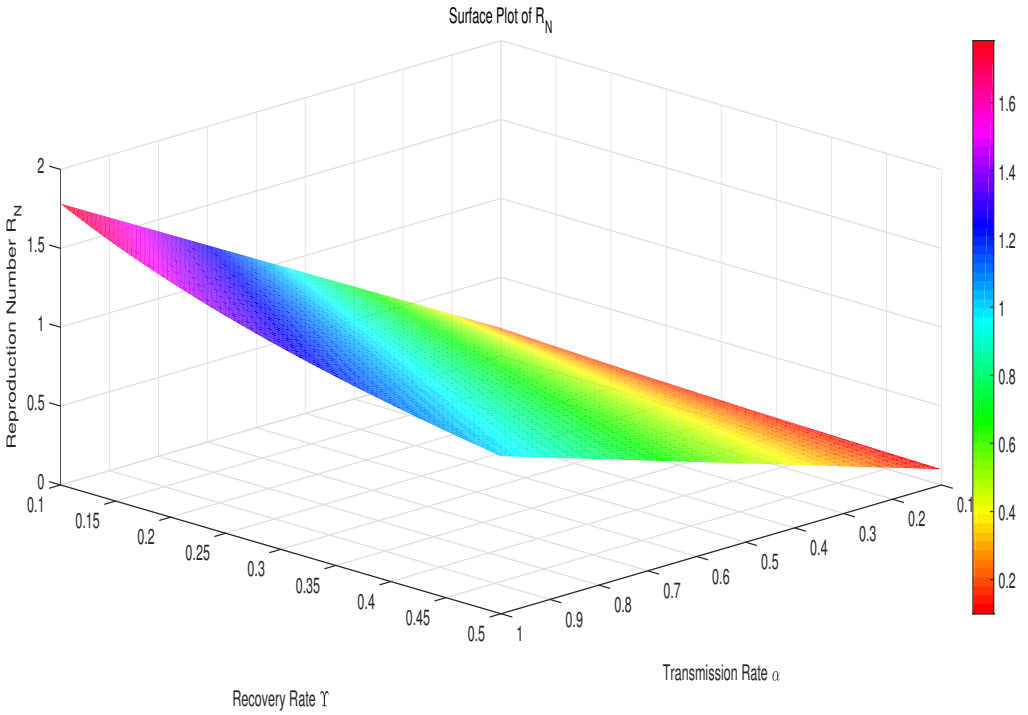

Figure 8: Three-dimensional plot illustrating the influence of transmission rate α and recovery rate Υ on the basic reproduction number R_N in the HBV model.

8. Conclusion

We analyzed the dynamics of HBV model that includes a Crowley-Martin perspective along with a fixed vaccination rate. By employing this incidence rate, we have accounted for both preventive measures by the susceptible HBV population and treatment concerning infectives, yielding more meaningful and realistic results compared to traditional saturated and bilinear incidence rates. Our study has established key properties of the hepatitis epidemic model, including the basic reproduction number, the boundedness and positivity of solutions, as well as stability characteristics and bifurcation behavior. We have demonstrated local asymptotic stability using the linear stability theorem and global asymptotic stability of the endemic equilibrium point using Dulac's criteria. The transcritical bifurcation has been confirmed at $R_N = 1$. Furthermore, in simulations, we have discretized the model using the NSFD scheme, ensuring dynamical consistency with the continuous model. Numerical simulations have validated our findings, highlighting the significance of the vaccination rate and disease transmission parameters in controlling the spread of HBV. Sensitivity analysis has further emphasized the importance of key parameters, revealing that the disease transmission rate (α) and recruitment rate (Ω) have the most positive impact on the basic reproduction number R_N, indicating that reducing transmission and limiting new infections are crucial in controlling the disease. Conversely, vaccination (Γ), preventive measures (η), and treatment parameters (Υ, κ, τ) contribute negatively to R_N, reinforcing their importance in mitigating HBV spread. The model can be used to inform public health policies aimed at controlling HBV transmission. By simulating different intervention strategies (e.g., vaccination campaigns, treatment programs), policymakers can evaluate the potential impact of these strategies on infection rates and overall public health. The limitations primarily stem from the assumptions in our model, such as constant vaccination rates and the use of the Crowley-Martin functional response, which may not fully capture real-world complexities. Additionally, parameter values are based on estimations, and real-world validation is needed. Future research could explore time-dependent vaccination strategies, incorporate more realistic transmission dynamics, and validate the model using epidemiological data. These extensions would enhance the model's applicability and predictive accuracy. Further, our next research will focus on the likelihood of reinfection

in individuals who have recovered from the hepatitis virus, especially as a Impact of unbalanced diets and negative lifestyle habits.

References

1. WHO, *World Health Organization Hepatitis B-Key Facts*. Available online: https://www.who.int/news-room/fact-sheets/detail/hepatitis-b
2. M.T. Hoang, O.F Egbelowo, *On the global asymptotic stability of a hepatitis B epidemic model and its solutions by nonstandard numerical schemes*, Bol. Sociedad Mat. Mex. 26(3), 1113–1134, (2024).
3. T. Khan, Z. Ullah, N. Ali, G. Zaman, *Modeling and control of the hepatitis B virus spreading using an epidemic model*, Chaos, Solitons Fractals, 124, 1–9, (2019).
4. V. Lavanchy, M. Kane, *Global Epidemiology of Hepatitis B Virus Infection*, Hepatitis B Virus in Human Diseases, 187–203, (2016).
5. B.O. Emerenini, S.C. Inyama, *Mathematical model and analysis of hepatitis B virus transmission dynamics*, F1000Research, 7, 1312, (2018).
6. WHO SJ, *World Health Organization (WHO) hepatitis B key facts*, (2020).
7. E.W. Hwang, R. Cheung, *Global epidemiology of hepatitis B virus (HBV) infection*, North American Journal of Medicine and Science, 4(1), 7-13, (2011).
8. World Health Organization, *Global policy report on the prevention and control of viral hepatitis in WHOMemberStates*, (2013).
9. A.S. Belay, D.D. Abateneh, S.S.Yehualashet, K.M. Kebede, *Hepatitis B virus infection and associated factors among adults in Southwest Ethiopia: community-based cross-sectional study*, Int. J. Gen. Med. 323-332, (2020).
10. Q.T. Ain, *Nonlinear stochastic cholera epidemic model under the influence of noise*, J. Math. Tech. Model. 1(1), 52–74, (2024).
11. M. Cornberg, V.W.S. Wong, S. Locarnini, M. Brunetto, H.L. Janssen, H.L.Y .Chan, *The role of quantitative hepatitis B surface antigen revisited*, J. Hepatol. 66(2), 398–411, (2017).
12. A. Din, *Bifurcation analysis of a delayed stochastic HBV epidemic model: cell-to-cell transmission*, Chaos Solitons Fractals, 181, 114714, (2024).
13. W.A. Khan, R. Zarin, A. Zeb, Y. Khan, A. Khan, *Navigating food allergy dynamics via a novel fractional mathematical model for antacid-induced allergies*, J. Math. Tech. Model, 1(1):25–51, (2024).
14. M.R.S Kulenovic, M. Nurkanovic, A. Yakubu, *Asymptotic behavior of a discrete-time density dependent SI epidemic model with constant recruitment*, J. Appl. Math. Comput. 67(1), 733–753, (2021).
15. A. Suryanto, W.M. Kusumawinahyu, I. Darti, and I. Yanti, *Dynamically consistent discrete epidemic model with modified saturated incidence rate*, Comput. Appl. Math. 32, 373–383, (2013).
16. World Health Organization, *Hepatitis B vaccines: WHO position paper, July 2017–Recommenda tions*, Vaccine, 37(2), 223-225, (2019).
17. K. Bruxvoort, J. Slezak, R. Huang, B. Ackerson, L.S. Sy, L. Qian, K. Reynolds, W. Towner, Z. Solano, Mercado C, and Hyer R, *Association of number of doses with hepatitis B vaccine series completion in US adults*, JAMA network open, 3(11), e2027577-e2027577, (2020).
18. A. Dwivedi, R. Keval, S. Khajanchi, *Modeling optimal vaccination strategy for dengue epidemic model: A case study of India*, Phys. Scr. 97: 085214, (2022).
19. AS. Lok, BJ. McMahon, *Chronic hepatitis B: update 2009*, Hepatology, 50(3), 661-662, (2009).
20. W.O. Kermack, A.G. McKendrick, *A contribution to the mathematical theory of epidemics*. Proc. R. Soc. Lond. 115(772), 700–721, (1927).
21. F. Brauer, C. Castillo-Chavez, *Mathematical Models in Population Biology and Epidemiology*, 2, Springer, New York, (2012).
22. U. Cakan, *Stability analysis of a mathematical model SIuIaQR for COVID-19 with the effect of contamination control (filiation) strategy*, Fundam. J. Math. Appl. 4(2):110–123, (2021).
23. Q. Cui, X. Yang, Q. Zhang, *An NSFD scheme for a class of SIR epidemic models with vaccina tion and treatment*, J. Differ. Equ. Appl. 20(3):416–422, (2014).
24. R.M Anderson, R.M. May, *Regulation and stability of host-parasite population interactions*, J. Anim.Ecol. 47(1), 219–247, (1978).
25. V. Capasso, G. Serio, *A generalization of the Kermack–McKendrick deterministic epidemic model*, Math. Biosci. 42(1-2):43–61, (1978).
26. J. Beddington, *Mutual interference between parasites or predators and its effect on searching effi ciency*, J. Anim. Ecol., 44(1), 331–340, (1975).

27. D.L. DeAngelis, R.A. Goldstein, R.V. O'Neill, *A model for tropic interaction*, Ecology, 56(4), 881-892, (1975).

28. A. Kaddar, On the dynamics of a delayed SIR epidemic model with a modified saturated incidence rate, Electr. j. differ. equ. 2009(133), 1–7, (2009).

29. A. Kaddar, Stability analysis in a delayed SIR epidemic model with a saturated incidence rate, Nonlinear Analysis: Modelling and Control, 15(3):299–306, (2010).

30. P.H. Crowley, E.K. Martin, *Functional responses and interference within and between year classes of a dragonfly population*, Journal of the North American Benthological Society, 8(3):211 221, (1989).

31. L.J. Allen, *An Introduction to Mathematical Biology Pearson Prentice Hall*, Upper Saddle River, New Jersey, (2007).

32. T.T. Yusuf, F. Benyah, Optimal control of vaccination and treatment for an SIR epidemiological model, World journal of modelling and simulation, 8(3):194–204, (2012).

33. M. Siva Pradeep, T. Nandha Gopal, A. Yasotha, *Dynamics and Bifurcation Analysis of an Eco Epidemiological Model in a Crowley–Martin Functional Response with the Impact of Fear*. Eng. Proc. 56:329, (2023). https://doi.org/10.3390/ASEC2023-16250

34. M. Thangavel, NG. Thangaraj, SP. Manickasundaram, Y. Arunachalam, *An Eco-Epidemiological Model Involving Prey Refuge and Prey Harvesting with Beddington–DeAngelis, Crow ley–Martin and Holling Type II Functional Responses*, Eng. Proc. 56(1), 325, (2023). https://doi.org/10.3390/ASEC2023-15812

35. I. Darti, A. Suryanto, *Dynamics of a SIR epidemic model of childhood diseases with a saturated incidence rate continuous model and its nonstandard finite difference discretization*, Mathematics, 8(9), 1459, (2020).

36. Z. Hu, Z. Teng, H. Jiang, *Stability analysis in a class of discrete SIRS epidemic models, Nonlinear Analysis: Real World Applications*, 13(5), 2017–2033, (2012).

37. R.E. Mickens, Nonstandard finite difference models of differential equations, world scientific, (1994).

38. R.E. Mickens, Nonstandard finite difference schemes: methodology and applications. World Scien tific, (2020).

39. J. Jaroszewicz, B.C. Serrano, K. Wursthorn, K. Deterding, J. Schlue, R. Raupach, R. Flisiak, C.T. Bock, M.P. Manns, H. Wedemeyer, and M. Cornberg, Hepatitis B surface antigen (HBsAg) levels in the natural history of hepatitis B virus (HBV)-infection: a European perspective, J. Hepatol. 52(4), 514-522, (2010).

40. P. Van den Driessche, J. Watmough, *Reproduction numbers and sub-threshold endemic equilibria for compartmental models of disease transmission*, Math. Biosci. 180(1), 29–48, (2002).

41. M. Gumus, K. Turk, *Dynamical behavior of a hepatitis B epidemic model and its NSFD scheme*, J. Appl. Math. Comput.1-22, (2024).

42. K. Hattaf, N. Yousfi, *A class of delayed viral infection models with general incidence rate and adaptive immune response*, Int. J. Dyn. Control. (2015).

43. H. El Mamouni, K. Hattaf, N. Yousfi, *Existence of traveling waves by means of fixed point theory for an epidemic model with Hattaf-Yousfi incidence rate and temporary immunity acquired by vaccination*, Adv. Fixed Point Theory (2023).

44. K. Hattaf, *A delayed SIR epidemic model with general incidence rate*, Electron. J. Qual. Theory Differ. Equ. (2013).

45. K. Hattaf, *A new class of generalized fractal and fractal-fractional derivatives with non-singular kernels*, Fractal and Fractional (2023)

46. K. Hattaf, *A new mixed fractional derivative with applications in computational biology*, Computation (2024).

47. T. Megala, T. Nandha Gopal, M. Siva Pradeep, et al. Dynamics of re-infection in a Hepatitis B Virus epidemic model with constant vaccination and preventive measures. J. Appl. Math. Comput. (2025). https://doi.org/10.1007/s12190-025-02431-1

Thangavel Megala,
Department of Mathematics,
Ramakrishna Mission Vidyalaya College of Arts and Science,
Coimbatore, India.
E-mail address: megala369@rmv.ac.in

and

Thangaraj Nandha Gopal,
Department of Mathematics,
Sri Ramakrishna Mission Vidyalaya College of Arts and Science,
Coimbatore, India.

E-mail address: nandhu792002@yahoo.co.in

and

Yasir Khan,
Department of Mathematics,
University of Hafr Al Batin, Hafr Al Batin,
Saudi Arabia.
E-mail address: yasirmath@yahoo.com

and

Manickasundaram Siva Pradeep,
Department of Mathematics,
United College of Arts and Science,
Coimbatore, India.
E-mail address: sivapradeep@rmv.ac.in

and

Muthuradhinam Sivabalan,
Department of Mathematics,
Sri Ramakrishna Mission Vidyalaya College of Arts and Science,
Coimbatore, India.
E-mail address: siva8890@gmail.com

and

Arunachalam Yasotha,
Department of Mathematics,
United College of Arts and Science,
Coimbatore, India.
E-mail address: yasotha@uit.ac.in